Mitochondrial Morphology Differences and Mitophagy Deficit in Murine Glaucomatous Optic Nerve

Lucy Coughlin,[1,2] Richard S. Morrison,[3] Philip J. Horner,[3] and Denise M. Inman[1]

[1]Department of Pharmaceutical Sciences, Northeast Ohio Medical University, Rootstown, Ohio, United States
[2]School of Biomedical Sciences, Kent State University, Kent, Ohio, United States
[3]Department of Neurological Surgery, University of Washington, Seattle, Washington, United States

Correspondence: Denise M. Inman, Northeast Ohio Medical University, 4209 State Route 44, Rootstown, OH 44272, USA; dinman@neomed.edu.

Submitted: November 22, 2014
Accepted: January 26, 2015

Citation: Coughlin L, Morrison RS, Horner PJ, Inman DM. Mitochondrial morphology differences and mitophagy deficit in murine glaucomatous optic nerve. *Invest Ophthalmol Vis Sci*. 2015;56:1437–1446. DOI:10.1167/iovs.14-16126

Purpose. Decreased ATP correlates with intraocular pressure exposure in the optic nerves of mice with glaucoma. To understand what underlies this energy deficit, we examined mitochondria in the myelinated optic nerve axons of the DBA/2J mouse, a model of glaucoma secondary to iris pigment disease, and the DBA/2$^{wt\text{-}gpnmb}$ control strain.

Methods. Mitochondrial length, width, surface area, and health status were measured in 30 electron microscopic fields within the myelinated portion of optic nerves from DBA/2J and DBA/2$^{wt\text{-}gpnmb}$ mice at 3, 6, and 10 months of age. Protein was isolated from optic nerve for analysis of PINK1, Parkin, LC3-I and -II, and lysosome-associated membrane protein 1 (LAMP1) by Western blot.

Results. The number of mitochondria in DBA/2J optic nerve was increased, and they had significantly smaller surface area. Mitochondria in DBA/2J were closer to the axolemma, more spatially isolated, and their cristae were more disrupted at every age group as compared to DBA/2$^{wt\text{-}gpnmb}$. Autophagosomes were significantly increased in DBA/2J optic nerve at all ages. Protein analysis showed higher LC3-II to LC3-I ratio in aged DBA/2J optic nerve than in DBA/2$^{wt\text{-}gpnmb}$. PINK1 and Parkin levels were not statistically different across age groups. LAMP1 was significantly decreased in the aged DBA/2J optic nerve.

Conclusions. Decreased surface area, combined with reduced oxidative capacity in mitochondria from the aged DBA/2J axon, indicate that mitochondrial pathology may contribute to the energy deficit in glaucomatous optic nerve. Though autophagosomes were increased in DBA/2J optic nerve, the increased mitochondria and decreased LAMP1 suggest deteriorating mitochondria are not being efficiently recycled by mitophagy.

Keywords: autophagosome, mitophagy, mitochondria

Changes in retinal ganglion cell function may be the earliest signs of glaucoma pathology in humans[1] and in the DBA/2J (D2) mouse model of secondary glaucoma. Pattern electroretinogram amplitude starts decreasing at 3 months of age in the D2 retina.[2] Decreased compound action potentials recorded from 6-month-old D2 optic nerve correlate with raised intraocular pressure (IOP).[3] An important step to understanding the mechanisms of glaucoma is to determine what causes these physiological impairments. A close correlation of decreased ATP levels with raised IOP could be a significant clue to the initiating pathology.[3] Mitochondria are the primary source of ATP in the central nervous system. Therefore, we sought to quantify changes in mitochondrial morphology and health in the optic nerves from D2 mice and their control strain, the DBA/2$^{wt\text{-}gpnmb}$ (D2-*Gpnmb*$^{+}$).

Neuronal mitochondria are functionally positioned in areas that require ATP or Ca^{2+} buffering.[4] Mitochondria are transported along microtubules in axons by using the energy-dependent molecular motors kinesin (anterograde) and dynein (retrograde). Declines in both anterograde and retrograde axon transport have been observed in the D2 model of glaucoma,[5–7] so if mitochondrial dysfunction can be demonstrated to precede these transport decreases, insufficient energy may explain the axon transport deficit.

Mitophagy is a regulated process by which dysfunctional mitochondria are recycled through the macroautophagy pathway. Mitochondria with inadequate membrane potential will fail to import PTEN-induced putative kinase 1 (PINK1) for degradation by PARL (presenilin-associated rhomboid-like) protease, allowing PINK1 to accumulate on the outer mitochondrial membrane.[8,9] PINK1 accumulation recruits Parkin, an E3 ubiquitin ligase. Parkin ubiquitinates outer mitochondrial membrane proteins and facilitates mitophagy. Mitophagy mediates mitochondrial quality control[10] and can take place locally in axons.[11] Mutations that impact mitophagy are associated with primary open-angle glaucoma (POAG). Optineurin is a cargo receptor for selective autophagy that brings an organelle for recycling into proximity with a phagophore, or recycling machinery.[12] Mutations in optineurin have been found in 16.7% of patients with hereditary POAG.[13] An optineurin mutation associated with amyotrophic lateral sclerosis prevents efficient mitophagy,[14] and a similar mechanism may explain the optineurin-mutation–associated cases of hereditary POAG.

This work tests the hypothesis that mitochondria underlie the metabolic vulnerability of the glaucomatous optic nerve. We show that mitochondria in optic nerve axons from DBA/2J mice are smaller, more numerous, and show more pathologic

Table. Number of Mitochondria Measured per Age Group Within Electron Micrographs of Myelinated Optic Nerve

Strain	Age, mo	Mitochondria
DBA/2J	3	665
	6	571
	10	479
DBA/2J$^{wt\text{-}gpmnb}$	3	1296
	6	1429
	10	1381

indices than age-matched control mice. Protein analysis indicates these mitochondria may be more numerous because they are not being efficiently recycled through mitophagy.

Materials and Methods

Mice

DBA/2J (D2) and DBA/2J$^{wt\text{-}gpmnb}$ (D2-*Gpnmb*$^{+}$) mice (Jackson Labs, Bar Harbor, ME, USA) were bred and housed at the University of Washington and Northeast Ohio Medical University. Intraocular pressure was monitored monthly by using the TonoLab (Tiolat Oy, Vantaa, Finland) rebound tonometer in mice that were lightly anesthetized with Avertin (0.5 mL/20 g of 1.8% 2,2,2-tribromoethanol, 0.3% *tert*-amyl alcohol, Sigma-Aldrich Corp., St. Louis, MO, USA). All procedures were approved by the Institutional Animal Care Committees of the University of Washington and Northeast Ohio Medical University and were performed in accordance with the ARVO Statement for the Use of Animals in Ophthalmic and Vision Research.

Electron Microscopy

Four mice each at 3, 6, and 10 months were used in the electron microscopic (EM) analysis for both D2 and D2-*Gpnmb*$^{+}$ strains. Optic nerves from each age group and each strain (see Table for number of mitochondria) were processed for electron microscopy. Mice were given an overdose of Beuthanasia-D (300 mg/kg sodium pentobarbital; Schering-Plough Animal Health, Kenilworth, NJ, USA) then transcardially perfused with 2% paraformaldehyde (PFA) plus 2% glutaraldehyde (Ted Pella, Redding, CA, USA) in 0.1 M sodium cacodylate buffer with 0.05% $CaCl_2$. Tissue was post fixed in 2% PFA plus 2% glutaraldehyde for 1 hour. After osmication in 1% OsO_4 (Ted Pella) for 1 hour, optic nerves were washed in 0.1 M phosphate buffer, dehydrated through an ascending alcohol series, then

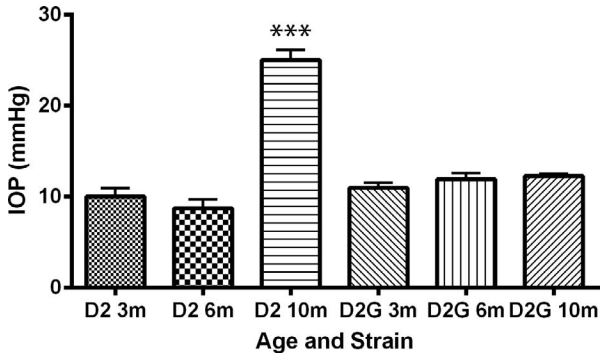

Figure 1. Final IOP measured in eyes used for EM, left and right eyes averaged together, $n = 4$ for each age group and strain. Final IOP for DBA/2 mice (D2) at 10 months is significantly greater than that of age-matched control (D2G) at 10 months; $^{***}P < 0.0001$. *Error bars*: SD.

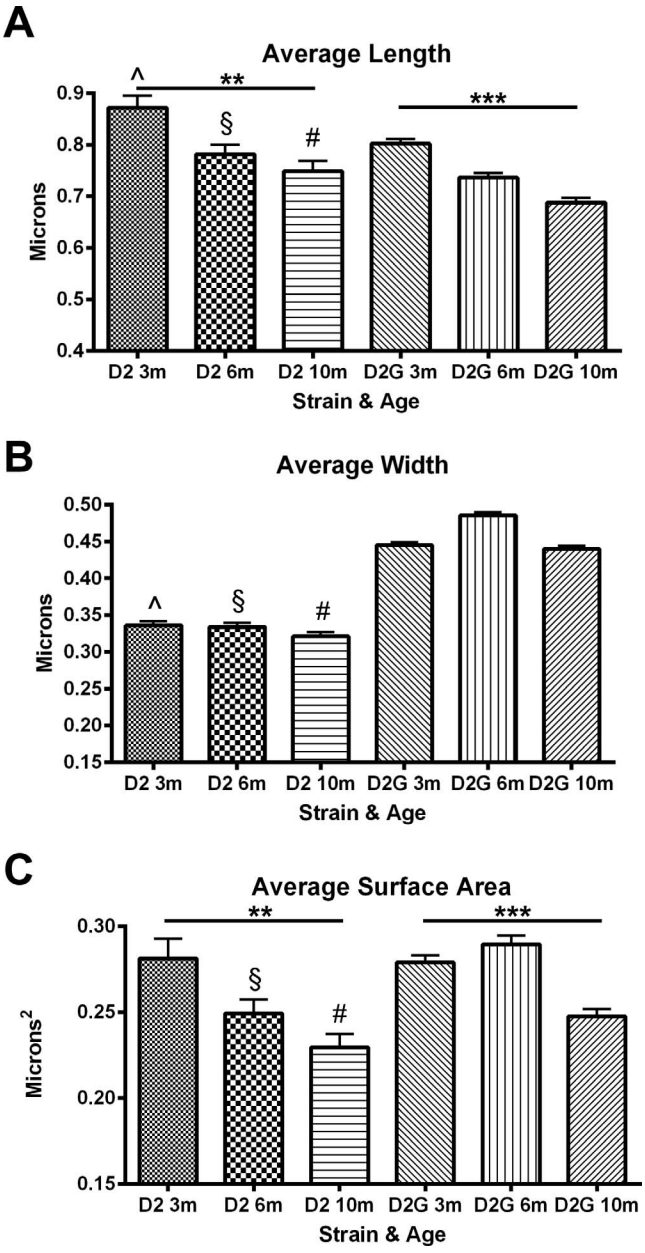

Figure 2. (**A**–**C**) Averaged mitochondrial measures in D2 versus D2G ON (optic nerve) at 3, 6 and 10 months of age. (**A**) Mitochondrial length decreased significantly with age in both D2 and D2G (ANOVA $^{**}P < 0.0055$ and $^{***}P < 0.0001$, respectively). *t*-tests indicate that each D2 length average is significantly greater than its corresponding D2G age group (3 months, $^{\wedge}P < 0.0011$; 6 months, $\S P < 0.028$; 10 months, $\#P < 0.0056$). (**B**) Mitochondria were significantly wider in D2G than D2 ON (*t*-test, 3 months, $^{\wedge}P < 0.0001$; 6 months, $\S P < 0.0001$; 10 months, $\#P < 0.0001$). (**C**) Mitochondrial area was calculated by using length, width, and the equation for area of an ellipse (see Methods). Average mitochondria area decreased significantly in D2 ON (ANOVA, $^{**}P < 0.0074$) and changed significantly in D2G ON (ANOVA, $^{***}P < 0.0001$). *t*-tests indicate that D2 area averages are significantly lower for D2G area at 6 months ($\S P < 0.0001$) and 10 months ($\#P < 0.04$). *Error bars*: SD.

washed twice in propylene oxide and subsequently embedded by using the Eponate 12 kit (Ted Pella). Ultrathin sections were cut at 60 nm on a Reichert Ultracut S microtome (Leica, Nussloch, Germany), mounted on nickel grids, and stained with uranyl acetate. Randomly chosen grids were then viewed with a Philips CM10 transmission electron microscope (TEM)

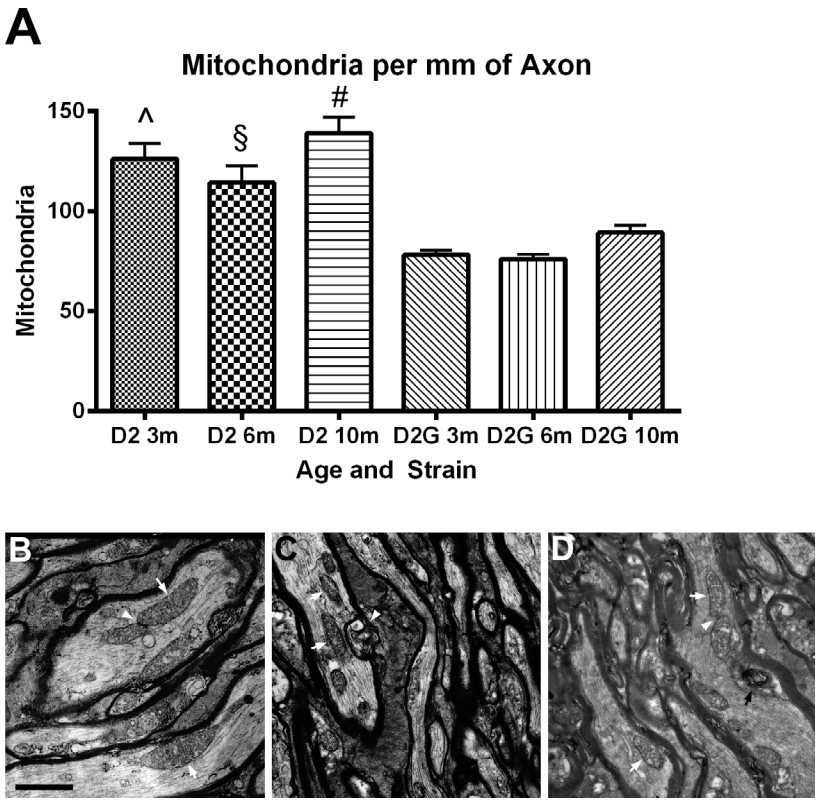

FIGURE 3. (**A**) D2 ON has significantly more mitochondria per millimeter of axon at each age group than D2G ON (*t*-tests, 3 months, ^$P < 0.001$; 6 months, §$P < 0.001$; 10 months, #$P < 0.001$). *Error bars* = SD. (**B–D**) D2 ON micrographs. *Scale bar*: 500 nm. (**B**) Three-month ON has abundant mitochondria (*arrows*) and an example of a possible fusion or fission event (*arrowhead*). (**C**) Six-month ON shows mitochondria (*arrows*) in close proximity to a multilamellar organelle, possibly an autophagic vacuole (*white arrowhead*). (**D**) Ten-month ON has mitochondria (*arrows*) and a possible fusion or fission event (*arrowhead*) not far from an autophagic vacuole (*black arrow*).

(Aachen, Germany) or a JEOL JEM 1200 EXII TEM (Tokyo, Japan) and photomicrographs taken. Micrographs were processed from the available technology, with images from the Philips CM10 TEM printed as film, while images from the JEM1200 TEM were saved as digital files.

Morphologic Analysis

Mitochondrial measurements were done by two blinded observers so that each mitochondrion was measured twice. The cumulative values from the individual observers did not differ statistically, so the values obtained by the primary observer are those reported here. Within each optic nerve, 30 to 40 150-μm^2 fields taken randomly from the myelinated portion of the optic nerve were analyzed. The Table shows the number of mitochondria analyzed per age and strain. Several mitochondrial parameters were measured on scanned EM negatives or digital EM images by using ImageJ (http://imagej.nih.gov/ij/; provided in the public domain by the National Institutes of Health, Bethesda, MD, USA). Pixel measurements were taken of mitochondria length, width, distance from the axon membrane, and distance to nearest neighbor (if applicable). The width values were from the widest point of the mitochondrion. The distance values were the shortest distances between mitochondrion and the axon membrane or its nearest neighbor. Only mitochondria within axons were measured. Measures were converted to micrometers by converting scan resolution dots per inch to dots per micrometer then multiplying by the magnification. An additional magnification correction factor was not used for output from either microscope because the difference between an imaged micrometer with microscope-stated versus microscope-calculated magnification was negligible (~2%). Surface area measures were calculated by using the equation for the area of an ellipse, $A = (Length/2) * (Width/2) * \pi$, where π is 3.142. Mitochondrial number is expressed as mitochondria per millimeter of axon in order to correct for the variable axon density within a 150-μm^2 electron microscopic field across ages and strains.

Mitochondrial cristae appearance was graded by using a five-point scale, 1 for the most degenerated or absent-appearing cristae and 5 for the most intact and well ordered. Observers were trained to use the scale and checked each other over one negative per animal to ensure conformity. See Figure 5 for the scale.

Protein Extraction and Western Blot Analysis

Protein was collected from optic nerves of freshly enucleated eyes from mice euthanized with Beuthanasia-D (Schering-Plough Animal Health). For each blot, optic nerves from two mice (four nerves total) from either strain at young (2- to 4-month-old) or old (9- to 11-month-old) time points were pooled into tubes containing lysis buffer (50 mM Tris HCl, 150 mM NaCl, 5 mM EDTA, and 1% Triton X-100) and protease inhibitor cocktail (Sigma-Aldrich Corp.), then disrupted with a Branson Sonifier (3-second pulse at 10% amplitude, Branson Ultrasonics Corp., Danbury, CT, USA) to create a protein lysate. Protein lysate (20 μg) was separated on denaturing polyacrylamide gels (SDS-PAGE) and transferred by electrophoresis to polyvinyl difluoride membrane (Bio-Rad, Hercules, CA, USA). The following antibodies were used for Western blot: β-actin

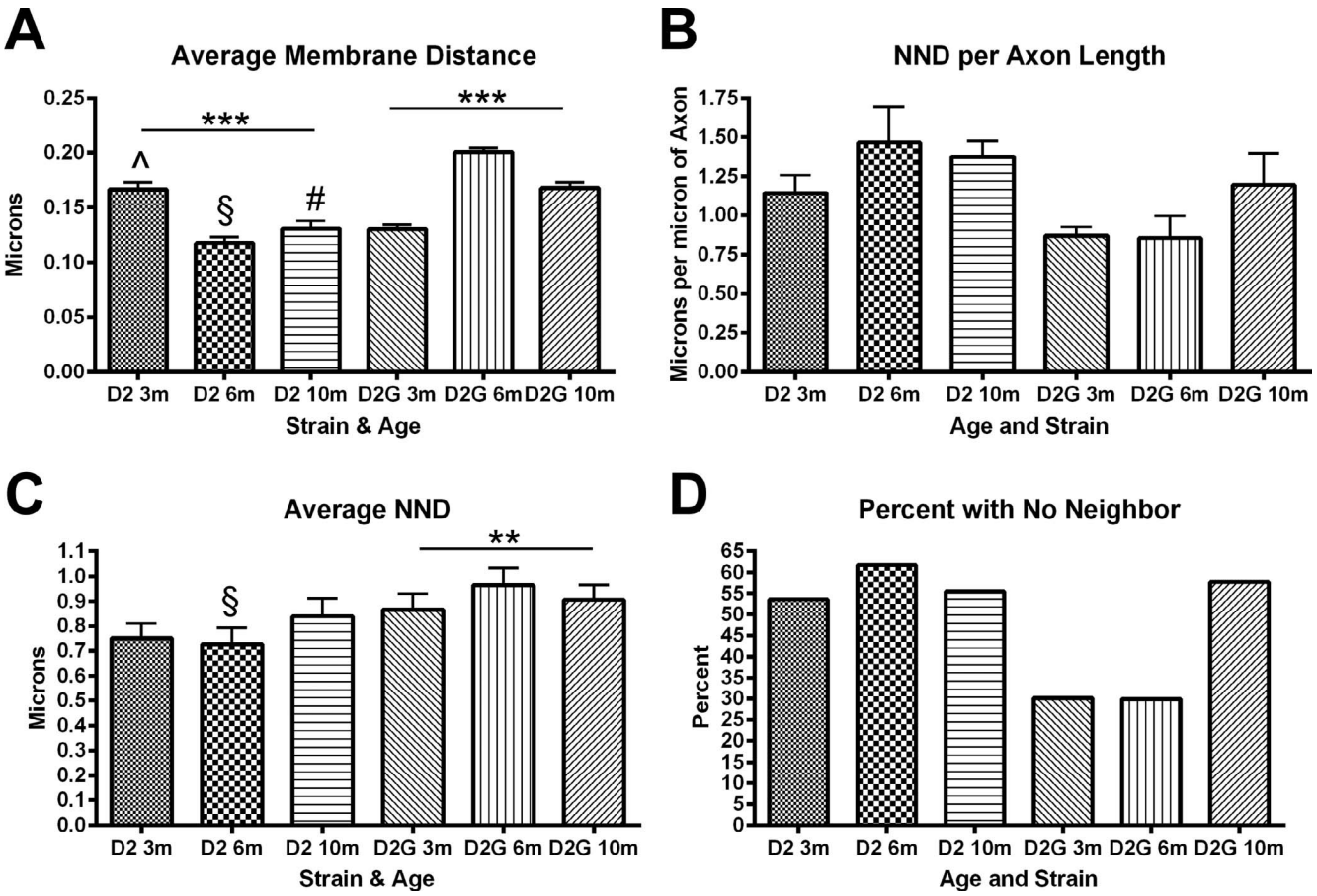

FIGURE 4. (**A**) Mitochondria undergo significant changes in distance from the axon membrane across age in both D2 and D2G ON (ANOVA, $^{***}P < 0.0001$). Membrane distance is significantly different at each age group in D2 versus D2G (*t*-tests, 3 months, $^{\wedge}P < 0.0001$; 6 months, $\S P < 0.0001$; 10 months, $\#P < 0.0001$). (**B**) Nearest neighbor distance, the distance between two mitochondria within an axon, varies across age and strain, but not in a statistically significant way. Data are represented as distance per micrometer of axon to correct for differences in axon length. (**C**) Average NND varies significantly across age in the D2G ON (ANOVA, $P = 0.0044$). At 6 months, NND is significantly lower in D2 ON (*t*-test, $P = 0.0123$). (**D**) More than 50% of D2 mitochondria were observed to be the only mitochondria within the axon in the EM field. D2G mitochondria have adjacent mitochondria 70% of the time until 10 months of age. *Error bars*: SD.

(1:1000; Abcam, Inc., Cambridge, MA, USA), PINK1 (1:1000; Cell Signaling, Beverly, MA, USA), Parkin (1:1000; Santa Cruz Biotechnology, Dallas, TX, USA), LC3A/B (1:2000; Cell Signaling), and lysosome-associated membrane protein 1 (LAMP1, 1:1000; Abcam). Blots incubated in primary antibodies (diluted at specified concentrations in Tris-buffered saline with 0.2% Tween-20 and 5% nonfat dried milk) were then exposed to the appropriate anti-rabbit or anti-mouse secondary antibodies conjugated to horseradish peroxidase (1:5000; Santa Cruz Biotechnology), developed with chemiluminescence (Thermo Fisher Scientific, Rockford, IL, USA), and exposed by using a Protein Simple gel doc imaging station (San Jose, CA, USA). Band density was measured by using the lane profile analysis function in AlphaView SA version 3.4.0 software (Protein Simple, San Jose, CA, USA) and was normalized to β-actin within lane band density. Expression is represented graphically as mean normalized value and standard error of the mean. At least three blots were run per antibody, with unique optic nerve homogenate from each age group for each run; hence, 24 mice were used per strain (DBA/2J and D2-*Gpnmb*$^{+}$) for the Western blot analysis.

Immunohistochemistry

Mice were injected with an overdose of Beuthanasia-D then perfused with 4% PFA in 0.1 M phosphate buffer. Eyes and attached optic nerves were dissected from the skull, and the anterior segment was separated from the posterior eyecup, which was then post fixed for 1 hour in 4% PFA. For sectioning, eyecups were rinsed in phosphate buffer (PB) (pH 7.4) and transferred to 30% sucrose in PB overnight. Eyecups were then embedded in OCT Tissue-Tek (Sakura Finetek, Torrance, CA, USA) and frozen in dry ice for sagittal sectioning on a Leica cryostat. The following antibodies were used for immunohistochemistry: LAMP1 (1:200; Abcam), NeuN (1:500; Millipore, Merck, Darmstadt, Germany). For immunohistochemistry, sections were blocked for 1 hour in 5% donkey serum plus 0.4% Triton X-100 then incubated overnight in primary antibodies. Tissue was rinsed, blocked for 30 minutes, and then incubated for 2 hours in appropriate secondary antibodies (anti–rabbit-AlexaFluor-594; anti–mouse-AlexaFluor-488; 1:250; Jackson ImmunoResearch Laboratories, Inc., West Grove, PA, USA). After rinsing, slides were mounted by using Fluoromount G (Southern Biotech, Birmingham, AL, USA). Images were captured with an Olympus confocal microscope (Olympus America, Central Valley, PA, USA).

Statistics

GraphPad Prism 6 (La Jolla, CA, USA) was used to perform one-way ANOVA (Kruskal-Wallis so as to not assume Gaussian distribution then Dunn's posttest when indicated by $P < 0.05$)

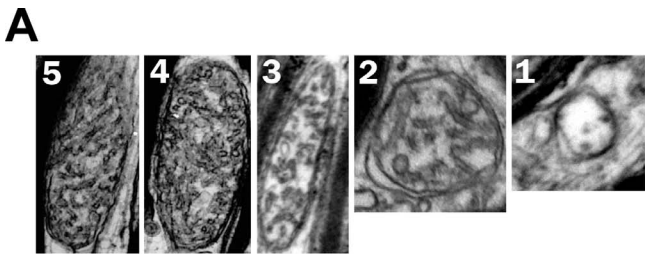

Grade	Condition
5	Intact, sharply defined, numerous and/or regular cristae
4	Occasional swollen cristae, slightly irregular
3	Fragmented and/or swollen cristae, irregularly packed
2	Severely fragmented or swollen cristae, warped membranes
1	Delamination of inner and outer mitochondrial membrane, absent cristae

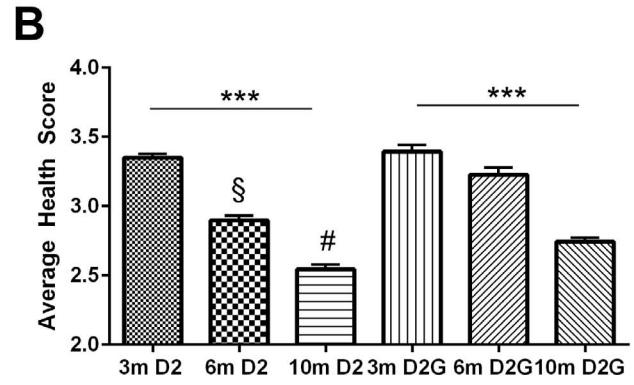

Figure 5. (**A**) Mitochondrial health scale is based primarily on cristae appearance. Grade of 5 is completely intact inner and outer membrane with regularly packed cristae. Grades 4 through 2 are decreasing levels of cristae preservation, and grade 1 represents missing cristae and breached inner or outer membrane. (**B**) Average health score for D2 glaucoma and D2G control ON mitochondria. Within-strain ANOVA indicates significant decrease in mitochondrial health from 3 to 10 months in both the D2 and the D2G (***$P < 0.0001$). Six-month D2 mitochondria have significantly poorer health scores than D2G (§$P < 0.0001$), as do 10-month D2 mitochondria (#$P < 0.0001$). *Error bars*: SD.

across age groups within strains and *t*-tests with Welch's correction for unequal variances to compare individual age groups across strains. Error bars are standard deviation except for Western blot analysis where error bars are standard error of the mean.

Results

Intraocular pressure was measured monthly. Averages of the final IOP for each mouse used in the EM analysis are shown in Figure 1. Ten-month D2 mice have significantly higher IOP than either age-matched D2-*Gpnmb*$^+$ control mice or 3- and 6-month D2 mice (*t*-test, $P < 0.0001$).

We made several morphologic measures of mitochondria in the myelinated portion of the D2 and D2-*Gpnmb*$^+$ optic nerve, including mitochondrial length and width in order to calculate surface area (see Methods). We counted mitochondria and measured axon length. Finally, we measured the distance between mitochondria and the distance of the mitochondria from the axon membrane. The Table shows the number of mitochondria measured by age and strain.

There was an overall decrease in mitochondrial length with aging; however, D2 mitochondria were significantly longer than D2-*Gpnmb*$^+$ mitochondria at each age (Fig. 2A). Interestingly, D2 mitochondria were significantly narrower than D2-*Gpnmb*$^+$ mitochondria at each age (Fig. 2B).

Mitochondrial surface areas varied significantly across time within strains, and despite D2s having longer mitochondria than D2-*Gpnmb*$^+$, D2 mitochondrial surface areas were significantly smaller than age-matched D2-*Gpnmb*$^+$ controls at 6 and 10 months: $P < 0.0001$ and $P < 0.04$, respectively (Fig. 2C). The decreases in D2 mitochondrial surface area amount to 13.9% and 7.2% smaller surface areas than the corresponding D2-*Gpnmb*$^+$ mitochondria.

There were significantly more mitochondria per millimeter of axon in the D2 optic nerve at every age. Interestingly, there was no age-related decrease in mitochondria number within the D2 or D2-*Gpnmb*$^+$ strains (Fig. 3A). Figures 3B through 3D show electron micrographs from D2 optic nerve at 3, 6, and 10 months. Multilamellar autophagic vesicles were apparent at 6 months (Fig. 3C, white arrowhead) and 10 months (Fig. 3D, black arrow) in the D2 optic nerve. In Figures 3B and 3D, arrowheads point to mitochondria in close proximity to each other, the scene of possible fusion or fission events.

The distance of mitochondria from the axon membrane varies, but in general decreases with aging in D2 (ANOVA, $P < 0.0001$). At each age, D2 mitochondrial distance from the membrane was significantly different from D2-*Gpnmb*$^+$ (Fig. 4A), with mitochondria at 6 and 10 months significantly closer to the axolemma in D2 than D2-*Gpnmb*$^+$ (*t*-tests, 3 months, ^$P < 0.0001$; 6 months, §$P < 0.0001$; 10 months, #$P < 0.0001$).

Nearest neighbor distance (NND), the distance between adjacent mitochondria, varied across ages and strains, but not in a statistically significant way when corrected for the length of the axon (Fig. 4B). Distance between mitochondria can suggest whether the mitochondria have undergone a recent fission event, thereby providing some measure of dynamism, since a mitochondrion alone in an axon would not likely have undergone recent fission. Mitochondria with adjacent mitochondria in the D2 optic nerve tend to be between 0.7 and 0.9 μm from each other (NND), regardless of age. In the D2-*Gpnmb*$^+$ optic nerve, distance between mitochondria varied significantly. However, only at 6 months were the NNDs significantly different between D2 and D2-*Gpnmb*$^+$ optic nerve ($P = 0.0123$; Fig. 4C). Nearest neighbor distance can only be measured in axons with more than one mitochondrion, so Figures 4B and 4C represent data from a subset of all mitochondria because more than 50% of D2 mitochondria are lone mitochondria in the axons of the EM fields assayed (a field is 150 μm^2) at every age (Fig. 4D). In contrast, roughly 70% of 3- and 6-month D2-*Gpnmb*$^+$ mitochondria had neighbor mitochondria, while that number dropped off to ~45% at 10 months (Fig. 4D).

A vital piece of contextual information to understand the mitochondrial morphology data is the relative health of the mitochondrion. To provide this context, we created a health scale from 1 to 5 (Fig. 5A), with 5 representing mitochondria of healthiest possible appearance (distinct and well-packed cristae, completely intact inner and outer membranes). Mitochondria health scores were assigned to all measured mitochondria. There was a significant age-related decrease in mitochondrial health regardless of strain (ANOVA, ***$P < 0.0001$). However, mitochondria in the D2 optic nerve at 6 and 10 months were significantly less healthy than mitochondria in the D2-*Gpnmb*$^+$ optic nerve (Fig. 5B, § and #).

The observations that D2 mitochondria were more numerous than the age-matched D2-*Gpnmb*$^+$, especially at 10 months of age, led us to examine whether deteriorating mitochondria in D2 optic nerve were not being recycled through the macroautophagy (mitophagy) pathway. Autophagosomes are the membrane-bound vesicles formed when organelles target-

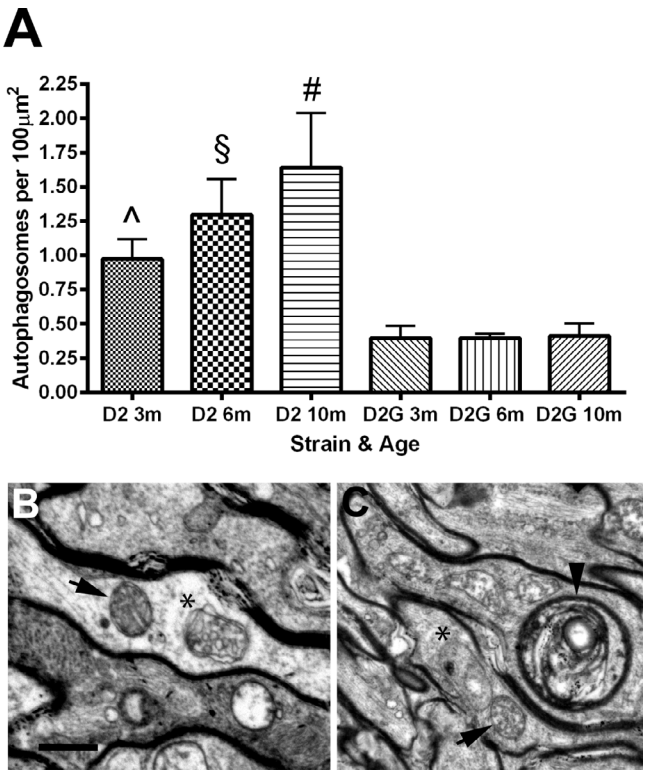

FIGURE 6. (**A**) Number of autophagosomes in axons per 100 μm² of optic nerve area. D2 ON has significantly greater numbers of autophagosomes than the age-matched D2G ON (two-tailed *t*-tests; 3 months, $^P < 0.01$; 6 months, $\S P < 0.005$; 10 months, $\#P < 0.03$). There is no statistical difference across age groups in the D2G ON. *Error bars* = SD. (**B**, **C**) Autophagosomes (*) adjacent to mitochondria (*black arrows*) in optic nerve. *Arrowhead* in (**C**) points to a multilamellar autophagic vesicle adjacent to multiple mitochondria (*above left*). *Scale bar*: 500 nm.

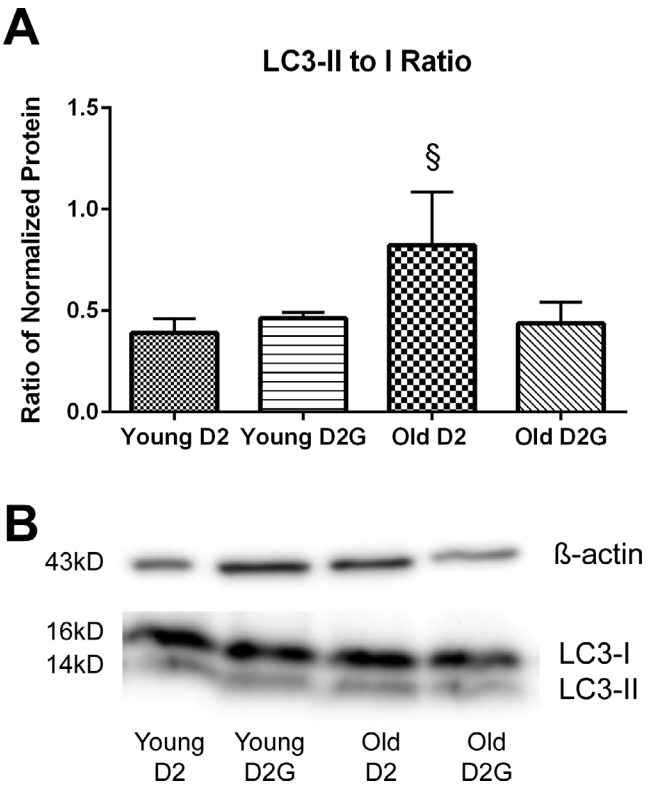

FIGURE 7. Ratio of LC3-II to LC3-I protein levels in D2 and D2G ON. LC3-I is conjugated to phosphatidylethanolamine to form LC3-II, and LC3-II remains with the autophagosome until lysosomal fusion. (**A**) The ratio of LC3-II to LC3-I is stable across young D2 and D2G ON and does not increase in old D2G ON (10 months). LC3-II to LC3-I ratio is significantly increased in old D2 ON ($\S P = 0.034$, *t*-test) compared to old D2G ON, indicating greater conjugation of LC3-I to LC3-II. *Scale bars*: SEM. (**B**) Representative immunoblot bands for LC3-I and LC3-II (*top*) and β-actin (*below*). Bands are in identical order to graphs.

ed for recycling are engulfed by membrane. Fusion of an autophagosome with a lysosome enables the contents to be broken down into amino acids for use elsewhere in the cell.[15] We quantified autophagosomes in D2 and D2-*Gpnmb*$^+$ optic nerve at each time point, finding significantly greater numbers of autophagosomes at every age in D2 optic nerve (Fig. 6A). There was a wide range of autophagosome-related double-membrane–bound organelles at the EM level, including immature autophagic vesicles and multilamellar autophagic bodies in the vicinity of mitochondria (Figs. 6B, 6C).

Increased autophagosome number could indicate increased autophagy initiation, decreased autophagic flux, or decreased autophagosome turnover. To begin to differentiate among these possibilities, we analyzed protein from freshly isolated optic nerve by Western blot in young (2–4 months of age) and old (9–11 months of age) D2 and D2-*Gpnmb*$^+$ mice. The conjugation of LC3-I to phosphatidylethanolamine (PE) to form LC3–PE conjugate (LC3-II) is a useful tool to monitor autophagy because LC3-II is recruited to the autophagosomal membrane and remains associated with it until fusion with the lysosome.[16] The ratio of LC3-II to LC3-I was significantly increased in old D2 optic nerve (Figs. 7A, 7B). Young and old D2-*Gpnmb*$^+$ optic nerve LC3-II to LC3-I ratio did not differ from young D2. The higher LC3-II to LC3-I ratio in old D2 optic nerve indicates greater conjugation of LC3-I to LC3-II, suggesting that autophagy induction is increased in old D2 optic nerve.

To understand whether there is increased mitophagy initiation in the D2 optic nerve, we measured protein levels of two mitophagy-associated proteins, PINK1 and Parkin. Neither PINK1 nor Parkin showed accumulation in the glaucomatous optic nerve (Figs. 8A–C; bands in panel D) contrary to expectation if there had been large numbers of mitochondria tagged for mitophagy. This indicates there is not increased mitophagy initiation in the old D2 optic nerve. The variability of PINK1 and Parkin proteins was high across the optic nerve at every time point, though old D2-*Gpnmb*$^+$ optic nerve had significantly lower levels of the 52-kDa Parkin isoform than young D2-*Gpnmb*$^+$ optic nerve (Fig. 8B).

For local mitochondrial recycling, lysosomes would be transported into the optic nerve axons from the retinal ganglion cell somata. Western blot of LAMP1 indicated significantly lower levels of LAMP1 in the old D2 optic nerve (Figs. 9A, 9B). Lower LAMP1 protein could indicate fewer lysosomes in the optic nerve, suggesting that the increased autophagosome number in the 10-month D2 optic nerve is due to decreased autophagosome turnover. LAMP1 immunolabeling of old D2 and D2-*Gpnmb*$^+$ retina showed high levels of LAMP1 in ganglion cell layer somata in both retinas (Fig. 9C).

DISCUSSION

Data obtained from electron micrographs of D2 and D2-*Gpnmb*$^+$ optic nerve at 3, 6, and 10 months of age showed that D2 optic nerve has significantly smaller (surface area) and less healthy mitochondria than those observed in D2-*Gpnmb*$^+$.

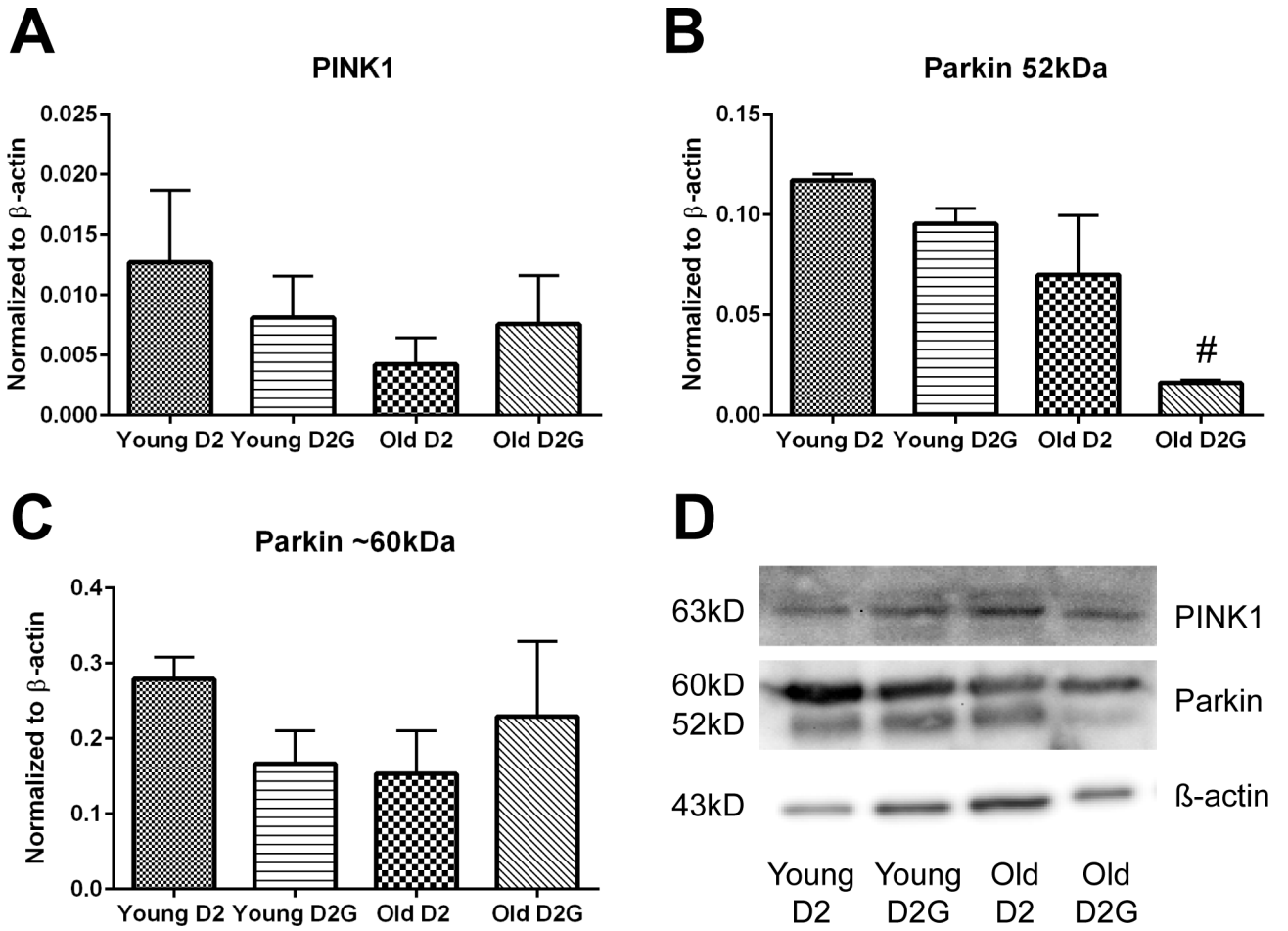

Figure 8. (**A**) PINK1 protein levels in young (2–4 months) and old (9–11 months) D2 and D2G ON. (**B**, **C**) Parkin protein levels in young and old D2 and D2G ON. There are several Parkin isoforms. Optic nerve homogenate yielded two bands, one at roughly 60 kDa and the other canonical band at 52 kDa. Parkin 60-kDa protein was significantly decreased in old D2G compared to young D2G ON (#$P = 0.0024$, *t*-test). *Error bars*: SEM (**A**–**C**). (**D**) Representative bands from immunoblots. Bands are in identical order to graphs.

Mitochondrial health was primarily determined by the appearance of the mitochondrial cristae. The electron transport chain and machinery for oxidative phosphorylation resides on the cristae in mitochondria. Cristae density and health serves as an indication of a mitochondrion's capacity for energy production.[17] A significant increase in unhealthy mitochondria in the 10-month D2 optic nerve indicates a compromised capacity for energy generation. This observation agrees with the finding of decreased mitochondrial respiration in lymphocyte samples from POAG patients.[18]

Regional mitochondrial number emerges from the balance of biogenesis, fusion and fission, and organelle recycling. A recent in situ hybridization analysis of PGC-1α in the D2 retina showed significant decreases in PGC-1α levels at 10 months compared to 1 and 5 months.[19] Low PGC-1α levels would limit mitochondrial biogenesis, suggesting that the high mitochondrial numbers in D2 optic nerve we observe are not due to increases in mitochondrial production. Pathologic triggers such as demyelination can trigger increases in mitochondrial mass,[20] as well as increases in the number of stationary mitochondria.[21] However, axon degeneration is not significant in the D2 optic nerve until beyond 10 months of age,[22] which indicates that mitochondrial changes at 3 and 6 months assayed here are upstream of axon breakdown.

Fusion and fission of mitochondria in response to cellular changes partially dictate mitochondrial number and mass. Opa1 is a membrane-anchored dynamin protein essential for mitochondrial fusion. Decreased Opa1 messenger RNA and protein, and shorter mitochondrial lengths, have been observed in the optic nerve head of the DBA2/J mouse.[23] Reduced Opa1, likely through proteolytic inactivation, prevents fusion of mitochondria, which are so damaged they do not have an inner membrane potential. Mitochondria respond to increased IOP by undergoing fission.[24] Interestingly, the D2 optic nerve mitochondria were significantly longer than in D2-*Gpnmb*$^{+}$, which may argue against increased fission, but their overall size (surface area) was significantly decreased. The timing of the differences (6 and 10 months) suggests the surface area decreases are the result of glaucomatous changes. The smaller surface areas (13.9% decrease at 6 months and 7.2% at 10 months) could indicate a change in the balance of mitochondrial dynamics toward fission, despite the longer mitochondrial lengths observed in the D2 optic nerve. Myelinated axons have pools of stationary and motile mitochondria[21,25]; the motile mitochondria can fuse with existing mitochondria, allowing them to compensate for mitochondrial DNA damage and alleviating the need for these organelles to travel great distances.[26] Postmitotic cells with an energy deficiency will make more mitochondria to compensate.[27] The smaller mitochondrial surface areas in 6- and 10-

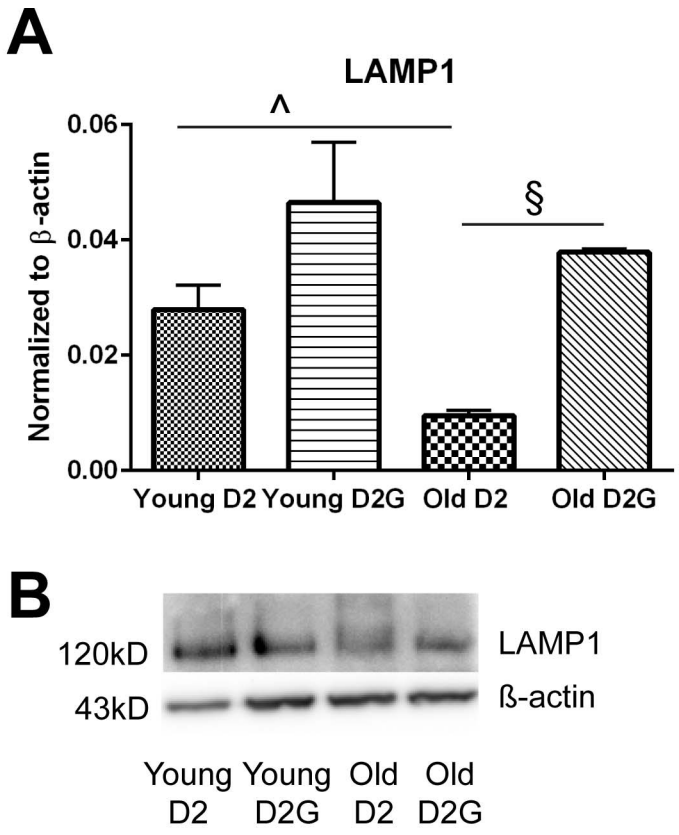

Figure 9. (**A**) Protein levels for LAMP1 in optic nerve. LAMP1 protein was significantly decreased in the old D2 ON compared to young D2 ON (^$P = 0.029$, *t*-test) and compared to old D2G ON (§$P = 0.0048$, *t*-test). *Scale bar*: SEM. (**B**) Representative bands from LAMP1 Western blot; *upper bands* are LAMP1 and *lower bands* are β-actin. Bands are in identical order to graphs. (**C**) Sagittal retinal sections from old (10–11 month) D2 and D2-*Gpnmb*$^+$ mice were immunolabeled with antibodies against NeuN (*green*) and LAMP1 (*red*). Photomicrographs depict the ganglion cell layer and inner plexiform layer. *Scale bars*: 25 μm.

month D2 optic nerve could indicate larger populations of motile mitochondria and lower levels of stationary mitochondria, though given the lower levels of PGC-1α in the aged D2 retina,[19] it is unlikely many motile mitochondria are coming from the retinal ganglion cells. The observations that D2 mitochondria have smaller surface area than the age-matched D2-*Gpnmb*$^+$, especially at 10 months of age, support the observations of others[24] that mitochondria undergo fission in response to increased IOP. Fission generates new mitochondria and facilitates recycling by segregating damaged mitochondria and targeting them for elimination.[28]

Lack of mitochondrial recycling, or mitophagy, might explain the high numbers of unhealthy mitochondria in D2 optic nerve. Autophagosomes observed in axons have been

Investigative Ophthalmology & Visual Science

shown to degrade mitochondria,[11] while basal autophagy serves primarily to degrade old proteins and organelles in the distal axon tips.[29] Interestingly, D2 optic nerve has a high incidence of autophagosome profiles. Since autophagosomes would be expected to recycle the high numbers of dysfunctional mitochondria found in aged D2 optic nerve, we investigated reasons why this may be compromised. Increased autophagosomes in the D2 optic nerve could result from increased induction of autophagy, reduction in autophagosome turnover, or the inability of turnover to keep pace with increased autophagosome formation. Our LC3-II to LC3-I data confirm increased autophagy induction in the glaucomatous optic nerve, also in agreement with an analysis of LC3 in a laser burn model of glaucoma in rat.[30] The stable PINK1 and Parkin protein levels nevertheless suggest that mitochondria are not being recycled in the aged D2 optic nerve. PINK1 accumulates on the outer mitochondrial membrane of mitochondria with inadequate membrane potential. Our mitochondrial health data predicted increased PINK1 levels in the aged D2 optic nerve. However, we observed PINK1 levels that were not statistically different across age and glaucoma and control strains. It may be the case that prospectively identified glaucomatous optic nerve would yield more consistent results. Also important to consider is that these protein analyses were undertaken in whole optic nerve, of which 28% of the volume is astrocytes and 38% is oligodendrocytes (including myelin).[31] Reduced mitophagy could also be the result of increased fusion/reduced fission, or failure of autophagosomes to encapsulate damaged mitochondria.

The LAMP1 data support decreased autophagosome turnover. If there are fewer lysosomes in the aged D2 optic nerve as the LAMP1 data suggest, there is decreased opportunity for local mitochondrial recycling. One potential mechanism for fewer lysosomes in the D2 optic nerve is the decreased anterograde axon transport that has been demonstrated in the D2 optic nerve by 9 to 10 months of age.[6,7] One might expect accumulation of lysosomes in the retinal ganglion cell soma if axon transport failure is preventing their movement into the optic nerve, but LAMP1 immunolabeling of the old D2 and D2-*Gpnmb*$^{+}$ retina did not indicate a difference. Future work will address lysosome number and enzyme activity in the optic nerve. Autophagosomes are retrogradely transported by the ATP-dependent dynein, like other axon cargo. ATP failure, as we have observed in the 10-month D2 optic nerve and in the 6-month D2 optic nerve with high IOP,[3] could explain accumulation of autophagosomes in the D2 optic nerve. If this were the case, axon transport deficit may emerge from mitochondrial metabolic dysfunction.

Astrocytes in unmyelinated optic nerve have been shown to engulf accumulations of intra-axonal debris, a process termed "trans-mitophagy."[32] Increased incidence of unhealthy mitochondria with small surface area in the 10-month D2 optic nerve suggest a breakdown of recycling and renewal. Though we observed significant numbers of autophagosomes in the D2 optic nerve, we were not able to confirm mitochondria were being tagged and engulfed by the autophagosomes. The lack of LAMP1 protein observed in the myelinated optic nerve could support the notion that intra-axonal debris needs to be transported to the optic nerve head for recycling. In our analysis of optic nerve, we did not observe any accumulations of intra-axonal debris and/or autophagosomes on the order of those observed with the transmitophagy analysis.[32] However, there are no data suggesting an accumulation threshold for transmitophagy, merely that it is has been observed in the optic nerve head and not the myelinated portion of the optic nerve.

We have not directly addressed the possibility of decreased autophagic flux in D2 optic nerve because of the difficulty in investigating flux in vivo. Altogether, our data suggest that autophagosomes are not able to contribute to organelle recycling because of the sparseness of LAMP1 in aged D2 optic nerve, so the autophagosomes are accumulating in the glaucomatous optic nerve. Whether mitochondria are within the accumulated autophagosomes is an ongoing investigation.

Acknowledgments

The authors thank Min Spencer of the University of Washington Center on Human Development and Disability for EM tissue processing and images; Jennifer M. Knox, Brian Buttrick, Liliana Bogin, David Kleesattel, and Pratyusha Muthineni for assistance with mitochondria morphology quantification; and Werner J. Geldenhuys for the generous gift of PINK1 and Parkin antibodies.

Supported by institutional funds to DMI, by National Institutes of Health Grant NS35533 to RSM, and by the Melza M. and Frank Theodore Barr Foundation through the Glaucoma Research Foundation to PJH. The authors alone are responsible for the content and writing of the paper.

Disclosure: **L. Coughlin**, None; **R.S. Morrison**, None; **P.J. Horner**, None; **D.M. Inman**, None

References

1. Banitt MR, Ventura LM, Feuer WJ, et al. Progressive loss of retinal ganglion cell function precedes structural loss by several years in glaucoma suspects. *Invest Ophthalmol Vis Sci*. 2013;54:2346–2352.
2. Saleh M, Nagaraju M, Porciatti V. Longitudinal evaluation of retinal ganglion cell function and IOP in the DBA/2J mouse model of glaucoma. *Invest Ophthalmol Vis Sci*. 2007;48:4564–4572.
3. Baltan S, Inman DM, Danilov C, Morrison RS, Calkins DJ, Horner PJ. Metabolic vulnerability disposes retinal ganglion cell axons to dysfunction in a model of glaucomatous degeneration. *J Neurosci*. 2010;30:5644–5652.
4. Zhang CL, Ho PL, Kintner DB, Sun D, Chiu SY. Activity-dependent regulation of mitochondrial motility by calcium and Na/K-ATPase at nodes of Ranvier of myelinated nerves. *J Neurosci*. 2010;30:3555–3566.
5. Buckingham BP, Inman DM, Lambert WS, et al. Progressive ganglion cell degeneration precedes neuronal loss in a mouse model of glaucoma. *J Neurosci*. 2008;28:2735–2744.
6. Crish SD, Sappington RM, Inman DM, Horner PJ, Calkins DJ. Distal axonopathy with structural persistence in glaucomatous neurodegeneration. *Proc Natl Acad Sci U S A*. 2010;107:5196–5201.
7. Dengler-Crish CM, Smith MA, Inman DM, Young JW, Wilson GN, Crish SD. Anterograde transport blockade precedes deficits in retrograde transport in the visual projection of the DBA/2J mouse model of glaucoma. *Front Neurosci*. 2014;8:290.
8. Matsuda N, Sato S, Shiba K, et al. PINK1 stabilized by mitochondrial depolarization recruits Parkin to damaged mitochondria and activates latent Parkin for mitophagy. *J Cell Biol*. 2010;189:211–221.
9. Narendra DP, Jin SM, Tanaka A, et al. PINK1 is selectively stabilized on impaired mitochondria to activate Parkin. *PLoS Biol*. 2010;8:e1000298.
10. Narendra D, Tanaka A, Suen D-F, Youle RJ. Parkin is recruited selectively to impaired mitochondria and promotes their autophagy. *J Cell Biol*. 2008;183:795–803.

11. Ashrafi G, Schlehe JS, LaVoie MJ, Schwarz TL. Mitophagy of damaged mitochondria occurs locally in distal neuronal axons and requires PINK1 and Parkin. *J Cell Biol*. 2014;206:655–670.
12. Randow F, Youle RJ. Self and nonself: how autophagy targets mitochondria and bacteria. *Cell Host Microbe*. 2014;15:403–411.
13. Rezaie T, Child A, Hitchings R, et al. Adult-onset primary open-angle glaucoma caused by mutations in optineurin. *Science*. 2002;295:1077–1079.
14. Wong YC, Holzbaur ELF. Optineurin is an autophagy receptor for damaged mitochondria in parkin-mediated mitophagy that is disrupted by an ALS-linked mutation. *Proc Natl Acad Sci U S A*. 2014;111:4439–4448.
15. Mizushima N, Komatsu M. Autophagy: renovation of cells and tissues. *Cell*. 2011;147:728–741.
16. Castillo K, Valenzuela V, Matus S, et al. Measurement of autophagy flux in the nervous system in vivo. *Cell Death Dis*. 2013;4:e917.
17. Perkins GA, Tjong J, Brown JM, et al. The micro-architecture of mitochondria at active zones: electron tomography reveals novel anchoring scaffolds and cristae structured for high-rate metabolism. *J Neurosci*. 2010;30:1015–1026.
18. Abu-Amero KK, Morales J, Bosley TM. Mitochondrial abnormalities in patients with primary open-angle glaucoma. *Invest Ophthalmol Vis Sci*. 2006;47:2533–2541.
19. Guo X, Dason ES, Zanon-Moreno V, et al. PGC-1α signaling coordinates susceptibility to metabolic and oxidative injury in the inner retina. *Am J Pathol*. 2014;184:1017–1029.
20. Zambonin JL, Zhao C, Ohno N, et al. Increased mitochondrial content in remyelinated axons: implications for multiple sclerosis. *Brain*. 2011;134(pt 7):1901–1913.
21. Kiryu-Seo S, Ohno N, Kidd GJ, Komuro H, Trapp BD. Demyelination increases axonal stationary mitochondrial size and the speed of axonal mitochondrial transport. *J Neurosci*. 2010;30:6658–6666.
22. Libby RT, Anderson MG, Pang I-HH, et al. Inherited glaucoma in DBA/2J mice: pertinent disease features for studying the neurodegeneration. *Vis Neurosci*. 2005;22:637–648.
23. Ju WK, Kim KY, Lindsey JD, et al. Intraocular pressure elevation induces mitochondrial fission and triggers OPA1 release in glaucomatous optic nerve. *Invest Ophthalmol Vis Sci*. 2008;49:4903–4911.
24. Ju WK, Liu Q, Kim KY, et al. Elevated hydrostatic pressure triggers mitochondrial fission and decreases cellular ATP in differentiated RGC-5 cells. *Invest Ophthalmol Vis Sci*. 2007;48:2145–2151.
25. Ohno N, Kidd GJ, Mahad D, et al. Myelination and axonal electrical activity modulate the distribution and motility of mitochondria at CNS nodes of Ranvier. *J Neurosci*. 2011;31:7249–7258.
26. Court FA, Coleman MP. Mitochondria as a central sensor for axonal degenerative stimuli. *Trends Neurosci*. 2012;35:364–372.
27. Wallace DC. A mitochondrial paradigm of metabolic and degenerative diseases, aging, and cancer: a dawn for evolutionary medicine. *Annu Rev Genet*. 2005;39:359–407.
28. Youle RJ, van der Bliek AM. Mitochondrial fission, fusion, and stress. *Science*. 2012;337:1062–1065.
29. Maday S, Wallace KE, Holzbaur ELF. Autophagosomes initiate distally and mature during transport toward the cell soma in primary neurons. *J Cell Biol*. 2012;196:407–417.
30. Kitaoka Y, Munemasa Y, Kojima K, Hirano A, Ueno S, Takagi H. Axonal protection by Nmnat3 overexpression with involvement of autophagy in optic nerve degeneration. *Cell Death Dis*. 2013;4:e860.
31. Perge JA, Koch K, Miller R, Sterling P, Balasubramanian V. How the optic nerve allocates space, energy capacity, and information. *J Neurosci*. 2009;29:7917–7928.
32. Davis C-HO, Kim K-Y, Bushong EA, et al. Transcellular degradation of axonal mitochondria. *Proc Natl Acad Sci U S A*. 2014;111:9633–9638.

Investigative Ophthalmology & Visual Science